

Three-body analysis of ^{11}Li and its β -decay to deuteron channel and to halo analog state $^{11}\text{Be}^*$ (18.3 MeV)

S KUMAR and V S BHASIN

Department of Physics and Astrophysics, University of Delhi, Delhi 110 007, India

MS received 26 September 2003; revised 27 March 2004; accepted 1 April 2004

Abstract. The ground state wave function of ^{11}Li obtained in a three-body model proposed earlier (S Kumar and V S Bhasin, *Phys. Rev.* **C65**, 034007 (2002)) has been employed to study the probability distributions, momentum distributions and n–n correlation. Complex scaling method has been used to find the energy positions and widths of the three resonant states of ^{11}Li above the breakup threshold. The formalism is extended further to study the β -decay of ^{11}Li to two channels. One is the β -transition of ^{11}Li into a high lying excited state of ^{11}Be at 18.3 MeV, i.e., $^{11}\text{Be}^*$ and the second is the decay to deuteron + ^9Li channel. The $^{11}\text{Be}^*$ state has been considered as a halo analog state identified as a bound three-body ($^9\text{Li} + n + p$) system. The n- ^9Li interaction incorporates both the virtual state and the p-wave resonance observed experimentally. For p- ^9Li interaction, a Coulomb corrected separable interaction is constructed using charge independence for strong interaction part. The n–p interaction is operative only in $^3\text{S}_1$ state corresponding to the isotopic spin $T_h = 0$. As a result the $^{11}\text{Be}^*$ state has the same isotopic spin as that of ^9Li core, i.e., $T = 3/2$. Using these realistic parameters as input and without invoking any other free parameter, the model has been used to predict the strength of the Gamow–Teller β -decay of ^{11}Li to $^{11}\text{Be}^*$, i.e., $B_{\text{GT}} = 1.5$ and the value of the branching ratio to $^9\text{Li} + \text{deuteron}$ channel to be 1.3×10^{-4} . These results are found to be in rather good agreement with the recent experimental findings.

Keywords. ^{11}Li ; neutron halo; β -decay; complex scaling method; n–n correlation.

PACS Nos 21.45.+v; 21.10.Dr; 21.60.Gx; 27.20.+n

1. Introduction

There have been numerous investigations [1–6] both on experimental and theoretical fronts in recent years on the halo structure of the ^{11}Li nucleus. Most of the experimental information on the neutron halo stems from the high energy reaction experiments involving ^{11}Li nucleus. It is now established that ^{11}Li can be considered as a three-body system consisting of ^9Li and the two valence neutrons. On the theoretical side, despite the fact that several attempts have been made so far to get

a deeper understanding of the two-neutron halo structure, the situation is still far from clear. Previous investigations [7–12] demonstrate the existence of both $(s_{1/2})^2$ and $(p_{1/2})^2$ components having about equal admixtures in the halo wave function. However, the recent experiments [13,14] carried out at ISOLDE on the β -decay of ^{11}Li suggest that the $(p_{1/2})^2$ component may not be the dominant one in the halo wave function.

We have recently carried out a study on the ground and excited states in continuum energy spectrum of ^{11}Li using a three-body model employing separable potentials for n–n and n– ^9Li interactions. Our analysis [15] also suggests a marginal role played by inclusion of p-state in n– ^9Li interaction. Here we wish to extend our study to investigate: (a) probability distributions, momentum distributions and n–n correlation in ground state of ^{11}Li , (b) energy position and widths of resonant states of ^{11}Li above breakup threshold, (c) β -decay of ^{11}Li to halo analog $^{11}\text{Be}^*$ (18.3 MeV) state, and (d) β -decay of ^{11}Li to deuteron + ^9Li channel. Experiments suggest that β -decay of ^{11}Li into a high lying state of the daughter nucleus $^{11}\text{Be}^*$ (18.3 MeV) is the super-allowed Gamow–Teller decay with reduced Gamow–Teller transition probability $B_{\text{GT}} > 1.0$. Such a large value of B_{GT} implies a large overlap of $^{11}\text{Be}^*$ state with the ground state of ^{11}Li . Following Zhukov *et al* [16], we have considered here $^{11}\text{Be}^*$ as the isobaric halo analog state consisting of ^9Li core with halo neutron–proton pair having isospin $T^h = 0$ and angular momentum $J^h = 1$.

In §2 we recapitulate the essential steps to write down the wave function of ^{11}Li as given in ref. [15] and outline the procedure to normalise the three-body wave function. The normalised wave function is used to study probability distribution, momentum distribution and n–n correlation. The results about excited resonant states of ^{11}Li using complex scaling method (CSM) are reported in §3. In §4, three-body wave function of halo analog $^{11}\text{Be}^*$ state is formulated on similar lines. In the next section we set up the formalism to calculate the B_{GT} value for the β -decay of ^{11}Li to $^{11}\text{Be}^*$ by computing the overlap between the parent and daughter nuclear states. The formalism has been extended further in §6 to calculate the branching ratio for the β -decay of ^{11}Li to deuteron + ^9Li channel. Finally §7 summarises the main results and specific features of the present approach.

2. Three-body model of ^{11}Li

Numbering the two valence neutrons and ^9Li core as particle numbers 1, 2, 3 respectively, we work in the centre of mass momentum space such that $\vec{p}_1 + \vec{p}_2 + \vec{p}_3 = 0$, thereby working with only two independent momenta. We choose the independent variables as \vec{p}_{12} , the relative momentum of particles 1 and 2 and \vec{p}_3 , the momentum of third particle with respect to the centre of mass of 1 and 2. All momenta are expressed in units of α/c where α is the deuteron binding energy parameter such that $(\alpha^2/m) = 2.226$ MeV, m being the nucleon mass and hence $\alpha = 45.7$ MeV and c is the speed of light. Also we use $\hbar = c = 1$ so that both energy and momentum can be expressed in units of α while solving the three-body system. In order to write down the three-body wave function of ^{11}Li , we employ the separable potentials for the binary subsystems n–n and n– ^9Li and choose for the n–n spin singlet $^1\text{S}_0$ interaction

Table 1. Parameters and observables of pairwise two-body interactions used in the three-body models for ^{11}Li and $^{11}\text{Be}^*$.

Binary system	Partial wave (l)	Strength parameter	Range parameter	Observables
n-n	0 (spin singlet)	$\lambda = 18.6\alpha^3$	$\beta = 5.8\alpha$	$a = -23.99$ fm $r = 2.32$ fm
n-p	0 (spin triplet)	$\lambda_{12} = 23.7\alpha^3$	$\beta_{12} = 5.5\alpha$	$a = 5.43$ fm $r = 1.90$ fm
n- ^9Li	0	$\lambda_0 = 2.25\alpha^3$	$\beta_0 = 3.0\alpha$	$a_s = -13.39$ fm $r_s = 4.93$ fm
n- ^9Li	1	$\lambda_1 = 2000.0\alpha^5$	$\beta_1 = 5.6\alpha$	$E_r = 0.538$ MeV $\Gamma = 0.475$ MeV
p- ^9Li	0	$\lambda_c^0 = 2.25\alpha^3$	$\beta_0 = 3.0\alpha$	$a_{sc} = -23.98$ fm $r_{sc} = 1.14$ fm
p- ^9Li	1	$\lambda_c^1 = 2000.0\alpha^5$	$\beta_1 = 5.6\alpha$	$E_r = 2.42$ MeV $\Gamma = 6.56$ MeV

$$\langle p'_{12} | V_{12} | p_{12} \rangle = -\frac{\lambda}{2\mu_{12}} g(p_{12}) g(p'_{12}), \quad g(p) = \frac{1}{p^2 + \beta^2}, \quad (1)$$

where strength parameter $\lambda = 18.6\alpha^3$ and the range parameter $\beta = 5.8\alpha$ are obtained so as to reproduce the n-n spin singlet scattering length $a = -23.69$ fm and effective range $r = 2.32$ fm. Similarly we choose the n- ^9Li separable potential in momentum space as

$$\langle \vec{p}'_{31} | V_{31} | \vec{p}_{31} \rangle = \sum_{l=0,1} (2l+1) V_{31}^l(p_{31}, p'_{31}) P_l(\cos \theta) \quad (2)$$

$$V_{31}^l(p_{31}, p'_{31}) = -\frac{\lambda_l}{2\mu_{31}} \nu_{31}^l(p_{31}) \nu_{31}^l(p'_{31}), \quad \nu_{31}^l(p) = \frac{p^l}{(p^2 + \beta_l^2)^{l+1}}, \quad (3)$$

with $l = 0, 1$ for the n-core (^9Li) interaction operative respectively in s- and p-states to reproduce a virtual $s_{1/2}$ state at an excitation energy of about 250 keV [17] and a p-wave resonance observed experimentally at $E_r = 0.538 \pm 0.062$ MeV with resonance width $\Gamma = 0.358 \pm 0.023$ MeV [18]. The range and strength parameters for these interactions are accordingly adjusted to reproduce these observables. These are summarised in table 1.

With these data in terms of two-body potentials we now write the three-body Schrödinger equation in momentum space as

$$(T - E)\Psi(\vec{p}_{12}, \vec{p}_3; E) = -\sum_{ij,k} \int \langle \vec{p}_{ij} | V_{ij} | \vec{p}'_{ij} \rangle \Psi(\vec{p}'_{ij}, \vec{p}'_k; E) d\vec{p}'_{ij}, \quad (4)$$

$$(ij, k) = (12, 3), (23, 1), (31, 2),$$

where T is the kinetic energy and E denotes the total energy in the three-body system and

$$T - E = \frac{p_{ij}^2}{2\mu_{ij}} + \frac{p_k^2}{2\mu_{ij-k}} - E \equiv D(\vec{p}_{ij}, \vec{p}_k; E) \quad (5)$$

$$\mu_{ij} = \frac{m_i m_j}{m_i + m_j}, \quad m_1 = m_2 = m = \text{nucleon mass}, m_3 = \text{mass of } ^9\text{Li core}$$

$$\mu_{ij-k} = \frac{(m_i + m_j)m_k}{m_i + m_j + m_k}, \quad p_{ij} = \frac{m_j p_i - m_i p_j}{m_i + m_j}.$$

Using the pairwise interactions given by eqs (1)–(3) in the three-body Schrödinger eq. (4), the analytical structure of the three-body wave function in the c.m. system can be written as

$$\Psi(\vec{p}_{12}, \vec{p}_3; E) = ND^{-1}(\vec{p}_{12}, \vec{p}_3; E) \begin{bmatrix} g(p_{12})G_1(p_3) + \nu_{23}^0(p_{23})G_2(p_1) \\ +\nu_{23}^1(p_{23})(\hat{p}_{23} \cdot \hat{p}_1)G_3(p_1) \\ +\nu_{31}^0(p_{31})G_4(p_2) \\ -\nu_{31}^1(p_{31})(\hat{p}_{31} \cdot \hat{p}_2)G_5(p_2) \end{bmatrix}. \quad (6)$$

The spectator functions $G_2(p_1)$ and $G_4(p_2)$ describe the dynamics of one halo neutron when the other halo neutron and the core are interacting through s-wave. Hence their structure is exactly the same. Similarly the functions $G_3(p_1)$ and $G_5(p_2)$ describe the dynamics of one neutron when the second neutron and core are interacting through p-wave. The function $G_1(p_3)$ represents the dynamics of ^9Li core in the presence of the two neutrons. In order to find a solution for these spectator functions we substitute the three-body wave function from eq. (6) back into the Schrödinger eq. (4) and compare the similar terms on two sides. This leads to a set of coupled integral equations that can be written in a closed form as

$$G_i(p) = \Lambda_i \left[h_i(p)G_i(p) + \sum_{j=1}^3 \int d\vec{q} K_{ij}(\vec{p}, \vec{q}; E)G_j(\vec{q}) \right], \quad i = 1, 2, 3. \quad (7)$$

The detailed structure of constants Λ_i , integrals h_i and kernels K_{ij} has been given in ref. [15]. To symmetrise the kernel in eq. (7), we use the following transformations:

$$G_1(p) \rightarrow \sqrt{2} \frac{\chi_1(p)}{p\sqrt{dp}} \sqrt{\Lambda_1}, \quad G_2(p) \rightarrow \frac{\chi_2(p)}{p\sqrt{dp}} \sqrt{\Lambda_2}, \quad G_3(p) \rightarrow \frac{\chi_3(p)}{p\sqrt{dp}} \sqrt{\Lambda_3}. \quad (8)$$

The final symmetric eigensystem can now be written as

$$\sum_{j=1}^3 \sum_q K'_{ij}(\vec{p}, \vec{q}; E)\chi_j(q) = \eta(E)\chi_i(p), \quad i = 1, 2, 3, \quad (9)$$

where we have introduced a parameter $\eta(E)$ which corresponds to the eigenvalue of the kernel of the above integral equation and $K'_{ij}(p, q; E)$ are the integral operators:

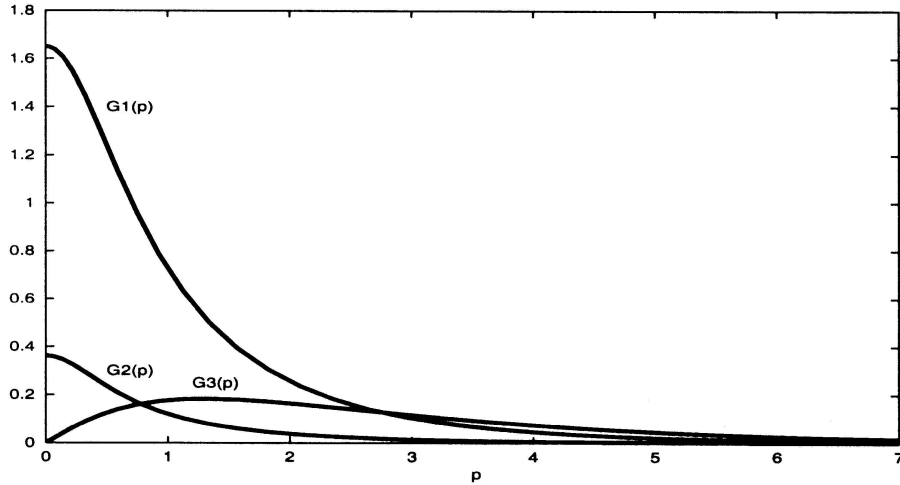


Figure 1. The spectator functions $G_1(p)$, $G_2(p)$ and $G_3(p)$ for ^{11}Li ground state. Here p along X -axis is in units of α .

$$K'_{ij}(p, q; E) = \Lambda_i h_i(p) \delta_{ij} \delta_{pq} + \sqrt{\Lambda_i \Lambda_j} \sqrt{dp dq} qp 2\pi \times \int_{-1}^{+1} d(\cos \theta) K_{ij}(\vec{p}, \vec{q}; E), \quad i, j = 1, 2, 3. \quad (10)$$

2.1 Ground state of ^{11}Li

The condition $\eta(E) = 1$ yields the solution of the above integral equation in the negative energy region and E corresponds to the bound state energy. Equation (9) has been numerically solved using Gauss quadrature to compute the three-body ground state energy and the momentum distribution of the spectator functions as eigenvectors. For the ground state of ^{11}Li obtained at energy $E = -0.286$ MeV, the plots of spectator functions vs. momentum are shown in figure 1. Also there is no excited bound state below the three-body breakup threshold in ^{11}Li .

Now in order to estimate the normalisation constant N of the three-body wave function subject to the condition

$$\int \Psi(\vec{p}_{12}, \vec{p}_3; E) \Psi^*(\vec{p}_{12}, \vec{p}_3; E) d\vec{p}_{12} d\vec{p}_3 = 1 \quad (11)$$

we note that, as a first step, we have to find out the analytical structure of these spectator functions which should accurately reproduce the numerical solutions as obtained by solving the integral equation. The analytical expressions which give the best fit are:

$$G_1(p) = \frac{A1}{1 + (p/p_0)^{A2}}, \quad A1 = 1.58\alpha^{-3}, \quad p_0 = 0.9131\alpha, \quad A2 = 2.121 \quad (12)$$

$$G_2(p) = G_4(p) = \frac{B1}{1 + (p/p_0)^{B2}}, \quad B1 = 0.343\alpha^{-3},$$

$$p_0 = 0.721\alpha, \quad B2 = 2.032 \quad (13)$$

$$G_3(p) = G_5(p) = A1 \left(1 - e^{-[p/A2]}\right)^{A4} e^{-[p/A3]}, \quad A1 = 0.62463\alpha \quad (14)$$

$$A2 = 1.37254\alpha, \quad A3 = 1.95298\alpha, \quad A4 = 1.13085. \quad (15)$$

With these algebraic representations for the spectator functions as input in the three-body wave function we then compute the quadrature of the integral in eq. (11) to evaluate the normalisation constant N , keeping the momentum vectors \vec{p}_{12} and \vec{p}_3 as basis to which all the other vectors such as \vec{p}_{31}, \vec{p}_2 etc. are properly transformed. The value of N comes out to be $0.0732\alpha^4$. The ground state wave function of ^{11}Li is thus completely known analytically and will be used to study the probability distribution, momentum distributions and β -decay to $^{11}\text{Be}^*$ state and $d + ^9\text{Li}$ channel.

2.2 Probability distribution in ^{11}Li

Defining

$$P(\vec{p}_{12}, \vec{p}_3) = \Psi(\vec{p}_{12}, \vec{p}_3; E) \Psi^*(\vec{p}_{12}, \vec{p}_3; E) \overrightarrow{dp_{12}} \overrightarrow{dp_3} \quad (16)$$

as the probability distribution of finding ^9Li with momentum p_3 in the volume element $p_3^2 dp_3 d\Omega_3$ and the correlation momentum p_{12} of the two halo neutrons in the element $p_{12}^2 dp_{12} d\Omega_{12}$, we can get some insight by plotting the probability density

$$\mathcal{P}(p_{12}, p_3) = p_{12}^2 p_3^2 \int d\Omega_{12} d\Omega_3 |\Psi(\vec{p}_{12}, \vec{p}_3)|^2 \quad (17)$$

versus the momenta p_{12} and p_3 in a three-dimensional plot shown in figure 2. In figures 3 and 4 we also depict the two-dimensional plots of the probability density against the momenta p_{12} and p_3 respectively (keeping the other momenta as fixed). The curves in figures 3 and 4 are those that pass through the peak in figure 2.

These figures show that the most probable values of momenta p_{12} and p_3 are 18.28 MeV/c and 30.16 MeV/c respectively. The FWHM (full-width at half-maximum), Γ_{12} in figure 3 is 27.42 MeV/c and by uncertainty principle this gives the most probable distance between the two halo neutrons as

$$r_{12} = r_{nm} = \frac{1}{\Gamma_{12}} = 7.19 \text{ fm}. \quad (18)$$

Similarly the FWHM, Γ_3 in figure 4 is 45.70 MeV/c which gives the most probable value of the distance of ^9Li core from the centre of mass of the two halo neutrons as

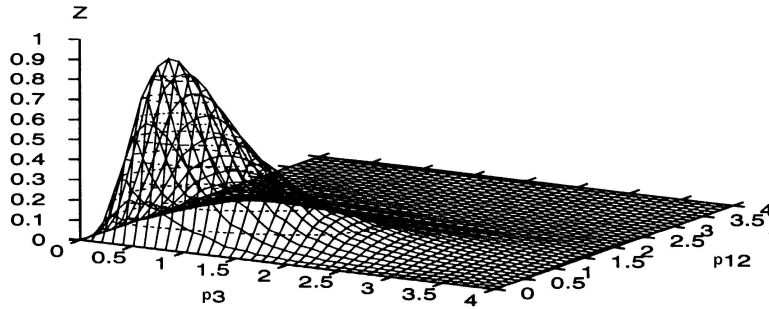


Figure 2. The probability density \mathcal{P} (along Z -axis) vs. p_{12} and p_3 . Here p_{12} and p_3 are in units of α .

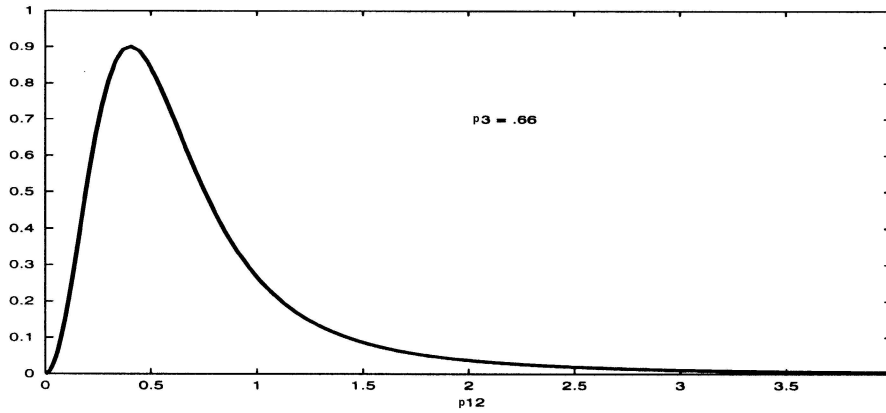


Figure 3. The probability density \mathcal{P} (along Y -axis) vs. p_{12} . Here p_{12} and p_3 are in units of α .

$$r_3 = r_{c-nn} = \frac{1}{\Gamma_3} = 4.32 \text{ fm.} \quad (19)$$

Having calculated r_{12} and r_3 from the three-body model, we can now estimate the rms radius, r_{matter} , of ^{11}Li using the relation

$$\langle r^2 \rangle_{\text{matter}} = \frac{A_c}{A} \langle r^2 \rangle_{\text{core}} + \frac{1}{A} \langle \rho^2 \rangle \quad (20)$$

originally given by Fedorov *et al* [19]. Here $\langle r^2 \rangle_{\text{core}}$ is the mean square value of the radius of ^9Li core and $\rho^2 = r_{12}^2 + r_3^2$. Taking the value of the ^9Li core radius to be 2.32 fm and substituting the values of r_{12} and r_3 from eqs (18) and (19) into eq. (20), we obtain the value of the matter radius of ^{11}Li to be 3.27 fm which is to be compared with the limits 3.2 ± 0.1 fm recently established by Garrido *et al* [20].

The study of the behaviour of probability amplitude with respect to the angle between vectors \vec{p}_{12} and \vec{p}_3 shows that the ground state of ^{11}Li has a maximum probability for a configuration when the n-n relative motion and the recoil motion of ^9Li are at right angle to each other in such a way that the halo neutrons when away from the core are closer and they are far away when closer to the core.

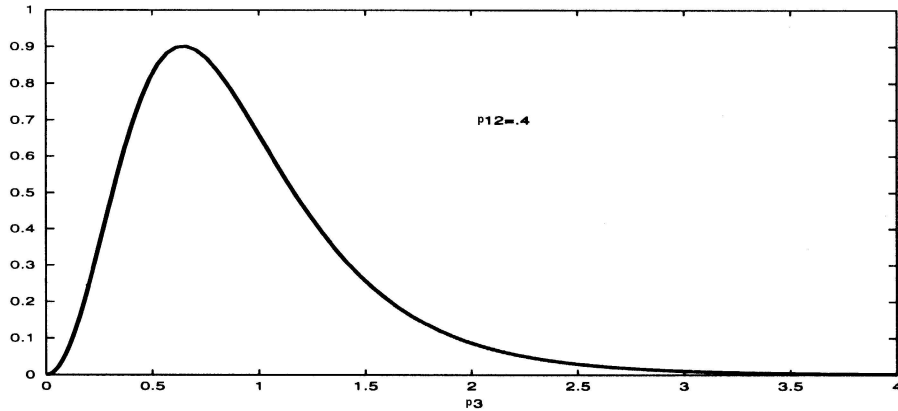


Figure 4. The probability density \mathcal{P} (along Y -axis) vs. p_3 . Here p_{12} and p_3 are in units of α .

2.3 n - n correlation in ^{11}Li from momentum distributions

One can also find the behaviour of longitudinal momentum distribution of ^9Li and that of the halo neutron by defining $\vec{p} = \vec{p}_{\parallel} + \vec{p}_{\perp}$. The longitudinal or parallel momentum distribution of ^9Li is by definition, the momentum distribution of ^9Li in the beam direction in fragmentation reaction of ^{11}Li beam on a target at certain beam energy. In the present model this implies that one should take \vec{p}_3 along beam direction only and integrate over the solid angle. Thus longitudinal momentum distribution of ^9Li in the present model is given by

$$\frac{dN}{dp_{3\parallel}} = \int dp_{12} d\Omega_{12} d\Omega_3 p_{12}^2 |\Psi(\vec{p}_{12}, \vec{p}_3)|^2. \quad (21)$$

This distribution which is compared with the latest experimental data [21] is shown in figure 5. Here the overall agreement with the experimental data shows that the inner structure of the ^9Li core has only a marginal role to play at large momenta in so far as the longitudinal component of the momentum distribution is considered. To derive the longitudinal momentum distribution of halo neutron, we first express the three-body wave function in terms of momentum vectors \vec{p}_{31} and \vec{p}_2 . Then the longitudinal momentum distribution of halo neutron is simply defined as

$$\frac{dN}{dp_{2\parallel}} = \int dp_{31} d\Omega_{31} d\Omega_2 p_{31}^2 |\Psi(\vec{p}_{31}, \vec{p}_2)|^2. \quad (22)$$

The longitudinal momentum distribution of halo neutron is shown in figure 6. However, the corresponding experimental data is not yet available to the best of our knowledge. From figure 5 the FWHM is estimated to be 46 MeV/c, which is in agreement with the experimental value of 45 ± 3 MeV/c [21]. In figure 6 FWHM is found to be 35 MeV/c for the halo neutron. Comparison of the two widths shows that

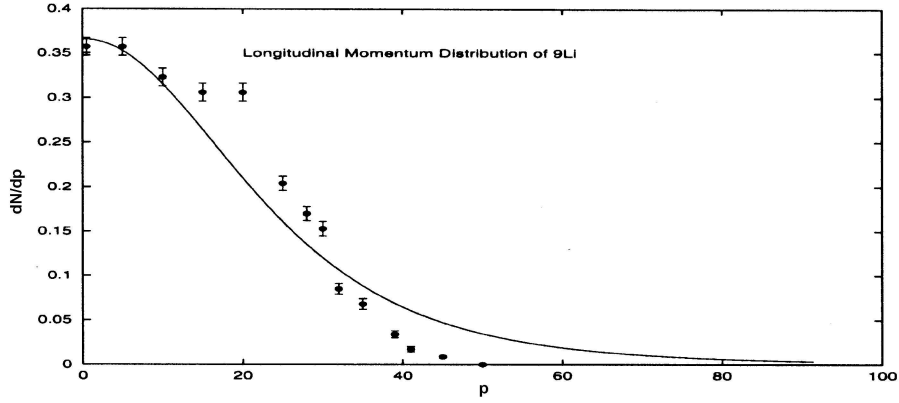


Figure 5. The longitudinal momentum distribution of ^9Li (along Y -axis) vs. $p_{3\parallel}$. Here $p_{3\parallel}$ is in MeV/c.

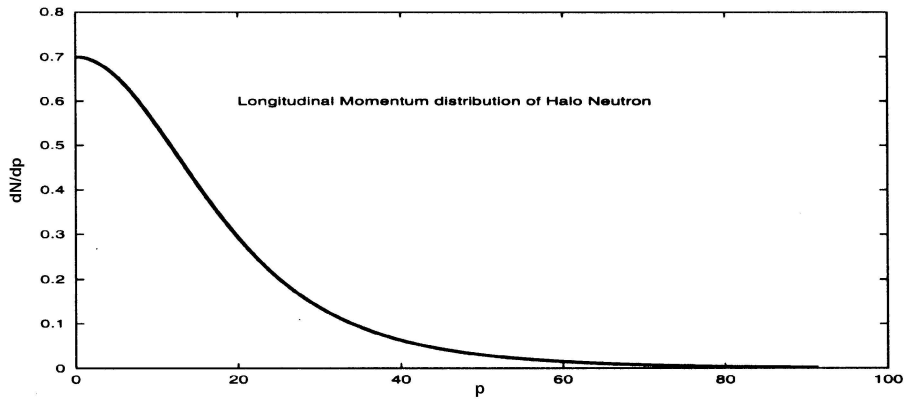


Figure 6. The longitudinal momentum distribution of halo neutron (along Y -axis) vs. $p_{2\parallel}$. Here $p_{2\parallel}$ is in MeV/c.

$$\frac{(\text{FWHM})_{^9\text{Li}}}{(\text{FWHM})_n} = 1.314 \quad (23)$$

which is only slightly less than the value for uncorrelated neutron pair, i.e., $\sqrt{2}$ [22]. It can thus be inferred that the two halo neutrons in ^{11}Li are nearly uncorrelated.

3. Resonant states of ^{11}Li above the three-body breakup threshold

For positive values of three-body energy E , the kernels of the integral eq. (9) in momentum space contain singularities on the real axis. In particular, there exists a range of p and q such that the kernel becomes a rapidly varying function of these variables. Hence the methods of bound states cannot be used here. A powerful method known as complex scaling method (CSM) has been recently developed (ref.

Table 2. Resonance states of ^{11}Li above the three-body breakup threshold.

No.	E_r (MeV) calculated	E_r (MeV) exp. data [23]	Γ (MeV) calculated
1	0.038	0.03 ± 0.04	0.056
2	1.064	1.02 ± 0.07	0.050
3	2.042	2.07 ± 0.12	0.500

[24] and references therein) for solving the many-body resonances and continuum states. In this method, the linear momenta (wave numbers) are transformed into complex numbers as

$$\vec{p} \longrightarrow \vec{p}e^{-i\theta}, \quad \vec{q} \longrightarrow \vec{q}e^{-i\theta}. \quad (24)$$

The resonance solutions are obtained as a complex energy: $E = E_r - i\Gamma$. The values of E_r and Γ are found to be independent of θ provided $\frac{1}{2} \tan^{-1}(\Gamma/2E_r) < \theta < \theta_c$. Here E_r is the resonance energy, Γ is the decay width and $\theta_c \approx 0.7$ is an upper bound on the value of θ . Thus in CSM, resonance states are treated in a way similar to the bound states. The first three resonant states of ^{11}Li with the values of the corresponding widths are given in table 2. The available experimental data on the resonance energies are also shown in table 2.

4. Wave function of halo analog $^{11}\text{Be}^*$ (18.3 MeV) state in a three-body ($^9\text{Li} + n + p$) model

Using the fact that the excess mass of ^{11}Be ground state is 20.174 MeV [25] and the excitation energy of $^{11}\text{Be}^*$ is 18.3 MeV, we get separation energy $E_{\text{sp}} = 1.8$ MeV relative to the $^9\text{Li} + n + p$ threshold in ^{11}Be . The $^{11}\text{Be}^*$ (18.3 MeV) state can thus be identified as a bound three-body ($^9\text{Li} + n + p$) system with binding energy of 1.8 MeV of the halo neutron and proton pair to the ^9Li core. To set up the three-body Schrödinger equation for $^{11}\text{Be}^*$ (18.3 MeV), we label the neutron, proton and the ^9Li core as particles 1, 2, and 3 respectively. The n- ^9Li interaction is the same as explained in the previous section. The additional problem in the study of p- ^9Li system is the handling of Coulomb interaction. The Coulomb potential is of course not separable and, at low energies, with particles held together in bound or resonant states as in halo nuclei, cannot be treated as a small perturbation. In this context Harrington [26] and Cattapan *et al* [27] have shown that the problem of determining the ‘Coulomb corrected’ phase shifts δ_{cl} due to a short range separable potential acting between two charged particles, is essentially the same as the corresponding problem with neutral particles. The effect of Coulomb potential is completely accounted for by the use of Coulomb modified functions V_{c23}^l rather than the original separable potential functions V_{23}^l . These potentials are written as

$$\langle \vec{p}_{23} | V_{23} | \vec{p}'_{23} \rangle = \sum_{l=0,1} (2l+1) V_{c23}^l(p_{23}, p'_{23}) P_l(\cos \theta), \quad (25)$$

$$V_{c23}^l(p_{23}, p'_{23}) = -\frac{\lambda_c^l}{2\mu_{23}} \nu_{c23}^l(p_{23}) \nu_{c23}^l(p'_{23}), \quad (26)$$

$$\nu_{c23}^l(p_{23}) = \nu_{23}^l(p_{23}) \frac{(2l+1)!}{(2l)!!} C_l(\eta) e^{2\eta \tan^{-1}(p_{23}/\beta_l)},$$

$$\nu_{23}^l(p) = \frac{p^l}{(p^2 + \beta_l^2)^2}, \quad (27)$$

$$C_l(\eta) = \frac{(l^2 + \eta^2)^{1/2}}{(2l+1)} C_{l-1}(\eta), \quad C_0(\eta) = \left[\frac{2\pi\eta}{e^{2\pi\eta} - 1} \right]^{1/2}, \quad \eta(k) = \frac{\mu e_1 e_2}{k}. \quad (28)$$

In eq. (28) e_1, e_2 denote the two charges, μ is the reduced mass and k is the wave number between the two particles.

In the case of p- ^9Li interaction, unfortunately, the experimental data, particularly at low energies are hardly available. We have therefore to resort to applying the hypothesis of charge independence and assume that the strong interaction part of p- ^9Li interaction is essentially the same as that of n- ^9Li system. With this proviso we can then use the parameters of n- ^9Li potential and predict the low energy observables as influenced by the presence of Coulomb force in p- ^9Li scattering. Employing the potential of eqs (25)–(28), we solve the Schrödinger equation for p- ^9Li system and compute the scattering amplitude both in s- and p-waves. From this we can then predict the values of the low energy observables for p- ^9Li scattering as scattering length $a_{sc} = -23.98$ fm and effective range $r_{sc} = 1.143$ fm in the case of s-state interaction while the position and width of the p-wave p- ^9Li resonance are found to be $E_r = 2.42$ MeV and $\Gamma = 6.56$ MeV. Thus it appears that Coulomb force plays a significant role at such low energies in so far as it affects the values of these observables considerably.

For Gamow–Teller β -decay of ^{11}Li involving the halo neutron pair in $T = 1$ and $S = 0$ state, one of the neutrons transforms to a proton resulting in the n-p pair in $T = 0$ and $S = 1$ state. For this 3S_1 spin triplet state of the halo neutron and proton pair we choose the separable potential

$$\langle \vec{p}'_{12} | V_{12} | \vec{p}_{12} \rangle = -\frac{\lambda_{12}}{2\mu_{12}} f(p_{12}) f(p'_{12}), \quad f(p) = \frac{1}{p^2 + \beta_{12}^2}. \quad (29)$$

The strength and the range parameters are adjusted to obtain the values of the scattering length $a = 5.43$ fm and range $r = 1.90$ fm deduced from the low energy scattering data [28]. All the binary interactions employed in the present work are summarised in table 1.

Substituting these potentials for n-n, n- ^9Li and p- ^9Li interactions in the three-body Schrödinger equation (4), we can read the structure of the three-body wave function as

$$\Psi_{11\text{Be}^*}(\vec{p}_{12}, \vec{p}_3; E) = N_1 D^{-1}(\vec{p}_{12}, \vec{p}_3; E) \begin{bmatrix} f(p_{12})H_1(p_3) \\ +\nu_{c23}^0(p_{23})H_2(p_1) \\ +\nu_{c23}^1(p_{23})(\hat{p}_{23} \cdot \hat{p}_1)H_3(p_1) \\ +\nu_{31}^0(p_{31})H_4(p_2) \\ +\nu_{31}^1(p_{31})(\hat{p}_{31} \cdot \hat{p}_2)H_5(p_2) \end{bmatrix}, \quad (30)$$

where, in eq. (30), $H_i(p)$ ($i = 1-5$) denote the spectator functions which describe the dynamics of the one particle in the presence of the other two mutually interacting particles. The dynamical structure of these functions can be obtained by substituting eq. (30) back into eq. (4) and comparing the corresponding terms on both sides. We thus obtain a set of five coupled integral equations involving the five spectator functions $H_i(p)$, which can be written in a concise manner as

$$H_i(p) = \Lambda_i \left[h_i(p)H_i(p) + \sum_{j=1}^5 \int d\vec{q} K_{ij}(\vec{p}, \vec{q}; E)H_j(\vec{q}) \right], \quad i = 1-5, \quad (31)$$

where

$$\Lambda_1 = \frac{\lambda_{12}}{2\mu_{12}}, \quad \Lambda_2 = \frac{\lambda_0}{2\mu_{31}}, \quad \Lambda_3 = \frac{\lambda_1}{2\mu_{31}}, \quad \Lambda_4 = \frac{\lambda_c^0}{2\mu_{23}}, \quad \Lambda_5 = \frac{\lambda_c^1}{2\mu_{23}}$$

and the elements of the kernel $K_{ij}(\vec{p}, \vec{q}; E)$ are written explicitly in Appendix 7. Before performing the numerical computation, the kernel of the integral in eq. (31) is symmetrised by using the transformation:

$$H_i(p) \longrightarrow \frac{\chi_i(p)}{p\sqrt{dp}} \sqrt{\Lambda_i}, \quad i = 1-5. \quad (32)$$

The final symmetric eigensystem can now be written by applying the suitable quadrature rule (Guass–Legendré) to eq. (31) as

$$\sum_{j=1}^5 \sum_q k'_{ij}(\vec{p}, \vec{q}; E)\chi_j(q) = \eta(E)\chi_i(p), \quad i = 1-5, \quad (33)$$

where we have introduced a parameter $\eta(E)$ which represents the eigenvalue of the above equation and $K'_{ij}(p, q; E)$ are the integral operators:

$$K'_{ij}(p, q; E) = \Lambda_i h_i(p)\delta_{ij}\delta_{pq} + \sqrt{\Lambda_i\Lambda_j} \sqrt{dp dq} \int_{-1}^{+1} d(\cos \theta) K_{ij}(\vec{p}, \vec{q}; E), \quad i, j = 1-5. \quad (34)$$

The numerical solution is achieved by use of the standard library routine ‘cg.f’ available on internet at EISPACK. The condition $\eta(E) = 1$ gives the solution for the three-body energy and the momentum distribution of the spectator functions as eigenvectors. We find that for the input parameters of the two-body potentials the resulting three-body system is somewhat overbound. Thus for instance using

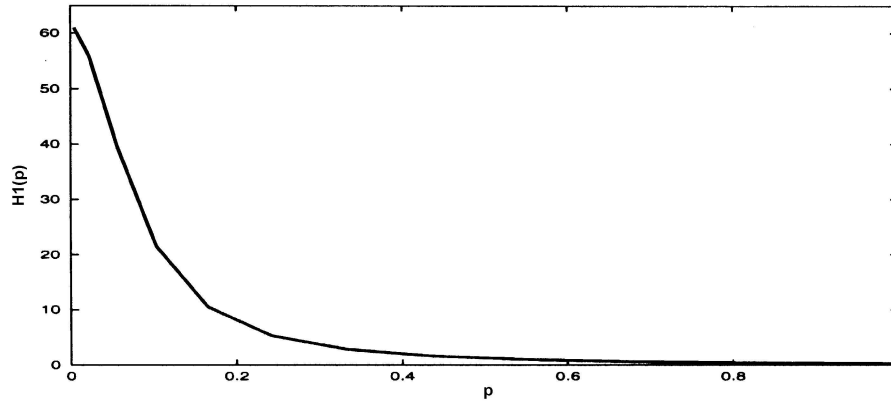


Figure 7. The spectator functions $H_1(p)$ vs. p for $^{11}\text{Be}^*$ excited state at 18.3 MeV. Here p along X -axis is in units of α .

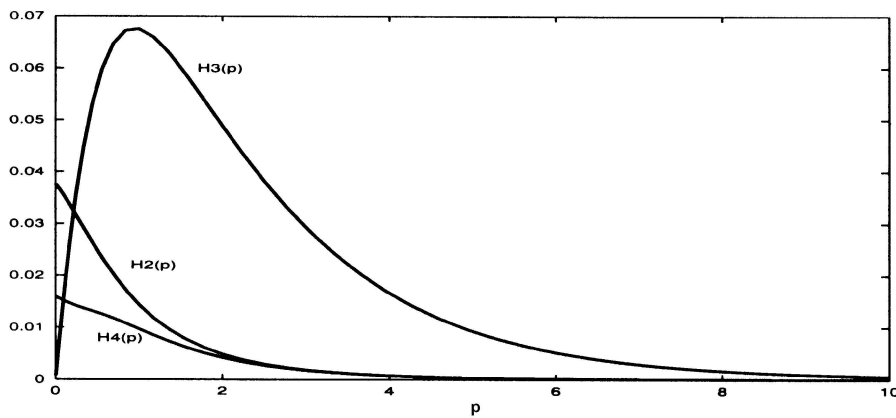


Figure 8. The spectator functions $H_2(p)$, $H_3(p)$, $H_4(p)$ vs. p for $^{11}\text{Be}^*$ excited state at 18.3 MeV. Here p along X -axis is in units of α .

the value of the spin triplet n - p strength parameter $\lambda_{12} = 23.7\alpha^3$ predicts the separation energy of the halo neutron-proton pair as 2.28 MeV instead of the required 1.8 MeV. This is possibly due to the fact that the binary n - p interaction does not include a small tensor component. It has however been found that if we reduce the strength parameter λ_{12} to $22.89\alpha^3$ (less than 3%) it can exactly reproduce the separation energy of the valence n - p pair as 1.8 MeV. For the $^{11}\text{Be}^*$ (18.3 MeV) state, the plots of spectator functions $H_i(p)$ ($i = 1-5$) are shown in figures 7-9.

As a next step in order to estimate the normalisation constant N_1 of the three-body wave function we first find out the analytical structure of the spectator functions which should accurately reproduce the numerical solution as obtained by solving the integral equation. The algebraic structures that give the best fit are

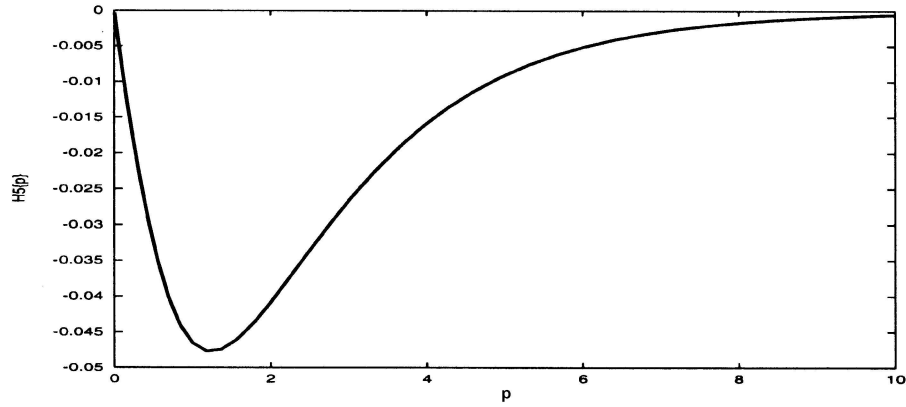


Figure 9. The spectator functions $H_5(p)$ vs. p for $^{11}\text{Be}^*$ excited state at 18.3 MeV. Here p along X -axis is in units of α .

$$H_1(p) = \frac{A1}{1 + (p/p_{01})^{A2}}, A1 = 60.920\alpha^{-3}, p_{01} = 0.0760\alpha, A2 = 2.020, \quad (35)$$

$$H_2(p) = \frac{B1}{1 + (p/p_{02})^{B2}}, B1 = 0.036\alpha^{-3}, p_{02} = 0.7647\alpha, B2 = 1.918, \quad (36)$$

$$H_3(p) = (C1 \times p) \times e^{-C2 \times p}, C1 = 0.179\alpha^{-3}, C2 = 0.974\alpha^{-1}, \quad (37)$$

$$H_4(p) = \frac{D1}{1 + (p/p_{03})^{D2}}, D1 = 0.015\alpha^{-3}, p_{03} = 0.7647\alpha, D2 = 2.259, \quad (38)$$

$$H_5(p) = (E1 \times p) \times e^{-E2 \times p}, E1 = -0.101\alpha^{-3}, E2 = 0.800\alpha^{-1}. \quad (39)$$

The three-body wave function is then normalised subject to the condition

$$\int \Psi_{^{11}\text{Be}^*}(\vec{p}_{12}, \vec{p}_3; E) \Psi_{^{11}\text{Be}^*}^*(\vec{p}_{12}, \vec{p}_3; E) d\vec{p}_{12} d\vec{p}_3 = 1. \quad (40)$$

Using the algebraic representations for the spectator functions given in eqs (35)–(39), we then compute the quadrature of the integral in eq. (40) and determine the value of the normalisation constant N_1 . The value of N_1 is found to be $0.157\alpha^4$.

5. β -Decay of ^{11}Li to halo analog $^{11}\text{Be}^*$ (18.3 MeV) state

Having equipped with the necessary details to write the complete three-body wave function for ^{11}Li and $^{11}\text{Be}^*$ states, we are now in a position to calculate the transition probabilities of β -decay of ^{11}Li to the different decay channels. Experimental studies [13,14,29,30] of β -delayed charged particles like deuterons, tritons, ^4He and ^9Be and neutrons and γ -rays that follow the ^{11}Li β -decay, indicates a β -feeding to an excited state at excitation energy of 18.3 MeV in ^{11}Be with a large Gamow–Teller strength, $B_{\text{GT}} \geq 1$. Now such a large value of B_{GT} implies a large spatial overlap of the $^{11}\text{Be}^*$ state and the ground state of ^{11}Li . Using the three-body wave

functions, obtained in the present approach, we calculate the value of the overlap integral, viz.

$$M_{fi} = \langle \Psi_{^{11}\text{Be}^*} | \Psi_{^{11}\text{Li}} \rangle = \int \Psi_{^{11}\text{Be}^*}^*(\vec{p}_{12}, \vec{p}_3; E) \Psi_{^{11}\text{Li}}(\vec{p}_{12}, \vec{p}_3; E) d\vec{p}_{12} d\vec{p}_3. \quad (41)$$

By substituting the wave functions given by eqs (30) and (6) we obtain the value to be 0.51. For Gamow–Teller β -decay of ^{11}Li involving the halo neutron pair in $T = 1$ and $S = 0$ state, when one of the neutrons transforms to a proton resulting in the n–p pair in $T = 0$ and $S = 1$ state, the spin triplet state has a statistical weight of 3. Since any of the two halo active neutrons may be undergoing β -decay, the total statistical factor should therefore be 6. Thus the reduced transition probability, B_{GT} , is defined as

$$B_{\text{GT}} = 6|M_{fi}|^2 \quad (42)$$

which in the present case gives the value of 1.5. This large value of Gamow–Teller strength appears to be in rather good agreement with the experimental findings. It is important to note that this is in fact a ‘parameter free’ prediction of the present model. As for the sensitivity of the detailed structure of ^{11}Li to β -decay, we find that the admixture of $(p_{1/2})^2$ configuration plays only a marginal role as is evident from the comparison of the spectator functions representing the neutron and ^9Li core in s- and p-states (see figure 1). This is also in qualitative agreement with the conclusions arrived at by Mukha *et al* [13] and Borge *et al* [14].

6. β -Decay of ^{11}Li to ^9Li + deuteron channel

As the next immediate application to check the sensitivity of the wave function of ^{11}Li we study β -decay of ^{11}Li to the d- ^9Li channel. The branching ratio for the deuteron channel decay $^{11}\text{Li} \rightarrow ^9\text{Li} + \text{d} + \bar{e} + \bar{\nu}$, for fixed initial and final states, per unit energy can be written as [16,31]

$$\frac{dB}{dE} = \frac{dW(^{11}\text{Li} \rightarrow ^9\text{Li} + \text{d} + \bar{e} + \bar{\nu})}{W(^{11}\text{Li} \rightarrow ^{11}\text{Be})dE}, \quad (43)$$

where

$$\frac{dW}{dE} = \left(\frac{G_\beta^2}{8\pi^5} \right) \left(\frac{m_e c^2}{\hbar^4} \right) (\mu k) f(Q - E) B_{\text{GT}}(E) \quad (44)$$

and

$$W = \left(\frac{G_\beta^2}{2\pi^3} \right) \left(\frac{m_e c^2}{\hbar} \right) \frac{ft(0^+ \rightarrow 0^+)}{t_{1/2}}. \quad (45)$$

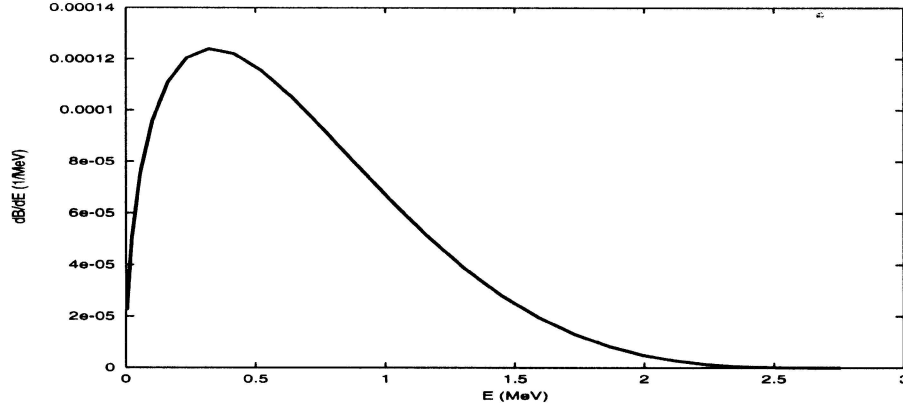


Figure 10. Energy spectrum of deuterons dB/dE (along Y -axis) vs. E . The peak is observed at around 0.32 MeV.

Substituting eqs (44) and (45) in eq. (43) we get the final expression for the branching ratio as

$$\frac{dB}{dE} = \frac{1}{4\pi^2} \frac{\mu k}{\hbar^3} \frac{B_{GT}(E) f(Q - E) t_{1/2}}{ft(0^+ \rightarrow 0^-)} \quad (46)$$

$$B_{GT}(E) = 6\lambda^2 \left| \int \Psi_d(\vec{p}_{12}) \Psi_f(k, \vec{p}_3) \Psi_i(\vec{p}_{12}, \vec{p}_3) \overrightarrow{dp}_{12} \overrightarrow{dp}_3 \right|^2. \quad (47)$$

In eqs (44) and (45), $t_{1/2} = 8.5$ ms is the β -decay half-life of ^{11}Li ; k is the wave number of the $^9\text{Li} + d$ channel at c.m. energy E ; μ is the reduced mass of the $^9\text{Li} + d$ system; $Q = 2.76$ MeV is the Q value for the decay of ^{11}Li to the $^9\text{Li} + d$ channel; $\lambda = -1.268$ is the ratio of the axial vector to the vector coupling constant; $f(Q - E)$ is the phase space (Fermi) integral for the deuteron channel and $ft(0^+ \rightarrow 0^-) = 3072.4$ s.

For the deuteron wave function we use the following standard wave function in momentum space as given in [32]:

$$\Psi_d(p_{12}) = \frac{\sqrt{\alpha\beta_1(\alpha + \beta_1)^3}}{\pi(p_{12}^2 + \beta_1^2)(p_{12}^2 + \alpha^2)}, \quad \beta_1 = 6.255\alpha, \quad (48)$$

where α is the deuteron binding energy parameter ($\alpha^2/m = 2.226$ MeV). For the initial state ^{11}Li wave function (Ψ_i) we use the normalised wave function of eq. (6). Here we consider only the direct decay to the deuteron continuum and assume that due to the low decay Q value (2.76 MeV), the relative d - ^9Li motion can be described only by s -wave. The general normalised scattering wave function for d - ^9Li relative motion can be written as

$$\Psi_f(\vec{p}_3) = \delta(\vec{p}_3 - \vec{k}) - \frac{1}{2\pi^2} \frac{f_k(p_3)}{k^2 - p_3^2 + i\epsilon} \quad (49)$$

where the delta function represents the plane wave part of the d- ^9Li relative motion and $f_k(p_3)$ denotes the off-shell scattering amplitude to take into account the final state interaction. For this purpose, we need to construct the scattering amplitude for d- ^9Li system in the presence of Coulomb interaction. As explained in §4, the effect of Coulomb potential is completely accounted for by the use of Coulomb modified functions $V_c(p_3)$ rather than the original separable potential functions $V(p_3)$. This Coulomb modified separable potential has been constructed similar to the case for p- ^9Li interaction in §4 and has been used to find the off-shell scattering amplitude appearing in eq. (49).

Thus using eq. (48) for deuteron wave function, eq. (49) for ^9Li -d wave function and eq. (6) for the three-body initial state of ^{11}Li , the overlap integral appearing in eq. (47) can be computed to find dB/dE . The plot of dB/dE vs. E is shown in figure 10 which depicts the maximum probability for deuterons being emitted at 0.32 MeV. Finally, the numerical integration of dB/dE over energy E gives us the total branching ratio to the deuteron channel which is found to be 1.3×10^{-4} . Clearly this value is in close agreement with the experimental value 1.5×10^{-4} reported in [13,14]. As pointed out in these references, the small discrepancy may be largely due to systematic error in experimentally detecting low energy deuterons indistinguishable from tritons.

7. Summary and conclusions

To summarise, we have here presented a three-body analysis studying the structural properties of ^{11}Li such as the ground state energy; the energy spectrum of first three resonant states above the three-body breakup threshold; the momentum distribution of the halo neutrons as well as that of the core; the n-n correlation and the separation of the core from the centre of mass of the halo neutrons in the nucleus. The matter radius of ^{11}Li has been calculated to be 3.27 fm which is in close agreement with the limits 3.2 ± 0.1 fm recently established by Garrido *et al* [20]. The three-body model has also been extended to study β -decay observables with a view to test the sensitivity of the three-body wave function. It predicts the B_{GT} value of 1.5 for β -decay of ^{11}Li to the $^{11}\text{Be}^*$ (18.3 MeV) state approximated as an isobaric halo analog state ($^9\text{Li} + n + p$). It may be mentioned that such an isobaric analog state of ^{11}Li in $^{11}\text{Be}^*$ was investigated by Teranishi *et al* [33] using charge exchange reaction $^{11}\text{Li}(p,n)^{11}\text{Be}^*$ in inverse kinematics at $E(^{11}\text{Li}) = 64$ A MeV. The branching ratio for β -decay to deuteron plus ^9Li channel is also found to be in good agreement with the experimentally observed value. We also find that the $(p_{1/2})^2$ components due to the p-state n- ^9Li interaction in the three-body wave function of ^{11}Li contribute marginally in reproducing the β -decay observables. The main assumptions in the present three-body model are: (a) to assume ^9Li core a structureless and spinless object and (b) to identify $^{11}\text{Be}^*$ (18.3 MeV) state as a composite of $^9\text{Li} + n + p$ configuration thereby neglecting some contributions from the complex structure of the ^{11}Be wave function in the excited state. Apparently, so long as we restrict ourselves to the low energy phenomena, the above effects would not significantly change the results of the present analysis. Nevertheless, these fine details need to be incorporated within the framework of a three-body approach in

the near future. It may however be emphasised that the present approach has the following distinct advantages: (i) It provides direct information about the momentum distribution of single particles within the nucleus through the knowledge of the spectator functions; (ii) the information about the two-body correlation can be obtained in a rather simple way from the solution of the three-body wave function and (iii) since the three-body observables are computed without resort to any approximation, any discrepancy between the calculated and observed quantity should directly reflect on the limitation of the input two-body potentials used.

Appendix A: Kernels of integral equations of $^{11}\text{Be}^*$

$$K_{12}(\vec{p}, \vec{q}; E) = \frac{V_{12}^0(|\vec{q} + \frac{\vec{p}}{2}|)V_{c23}^0(|-\vec{q} - \frac{m_3}{m+m_3}\vec{p} - \vec{p}|)}{(\frac{q^2}{m} + \frac{\vec{q}\cdot\vec{p}}{m} + \frac{p^2}{2\mu_{mm_3}} - E)} \quad (\text{A1})$$

$$K_{13}(\vec{p}, \vec{q}; E) = -\frac{V_{12}^0(|\vec{q} + \frac{\vec{p}}{2}|)V_{c23}^1(|-\vec{q} - \frac{m_3}{m+m_3}\vec{p} - \vec{p}|)}{(\frac{q^2}{m} + \frac{\vec{q}\cdot\vec{p}}{m} + \frac{p^2}{2\mu_{mm_3}} - E)}\Delta_1 \quad (\text{A2})$$

$$K_{14}(\vec{p}, \vec{q}; E) = \frac{V_{12}^0(|-\vec{q} - \frac{\vec{p}}{2}|)V_{31}^0(|\vec{q} - \frac{m_3}{m+m_3}\vec{p} + \vec{p}|)}{(\frac{q^2}{m} + \frac{\vec{q}\cdot\vec{p}}{m} + \frac{p^2}{2\mu_{mm_3}} - E)} \quad (\text{A3})$$

$$K_{15}(\vec{p}, \vec{q}; E) = \frac{V_{12}^0(|-\vec{q} - \frac{\vec{p}}{2}|)V_{31}^1(|\vec{q} - \frac{m_3}{m+m_3}\vec{p} + \vec{p}|)}{(\frac{q^2}{m} + \frac{\vec{q}\cdot\vec{p}}{m} + \frac{p^2}{2\mu_{mm_3}} - E)}\Delta_1 \quad (\text{A4})$$

$$K_{42}(\vec{p}, \vec{q}; E) = \frac{V_{31}^0(|-\vec{q} - \frac{m}{m+m_3}\vec{p}|)V_{c23}^0(|\vec{q} - \frac{m}{m+m_3}\vec{p} + \vec{p}|)}{(\frac{q^2}{2\mu_{mm_3}} + \frac{\vec{q}\cdot\vec{p}}{m_3} + \frac{p^2}{2\mu_{mm_3}} - E)} \quad (\text{A5})$$

$$K_{43}(\vec{p}, \vec{q}; E) = \frac{V_{31}^0(|-\vec{q} - \frac{m}{m+m_3}\vec{p}|)V_{c23}^1(|\vec{q} - \frac{m}{m+m_3}\vec{p} + \vec{p}|)}{(\frac{q^2}{2\mu_{mm_3}} + \frac{\vec{q}\cdot\vec{p}}{m_3} + \frac{p^2}{2\mu_{mm_3}} - E)}\Delta_2 \quad (\text{A6})$$

$$K_{52}(\vec{p}, \vec{q}; E) = -\frac{V_{31}^1(|-\vec{q} - \frac{m}{m+m_3}\vec{p}|)V_{c23}^0(|\vec{q} - \frac{m}{m+m_3}\vec{p} + \vec{p}|)}{(\frac{q^2}{2\mu_{mm_3}} + \frac{\vec{q}\cdot\vec{p}}{m_3} + \frac{p^2}{2\mu_{mm_3}} - E)}\Delta_3 \quad (\text{A7})$$

$$K_{53}(\vec{p}, \vec{q}; E) = -\frac{V_{31}^1(|-\vec{q} - \frac{m}{m+m_3}\vec{p}|)V_{c23}^1(|\vec{q} - \frac{m}{m+m_3}\vec{p} + \vec{p}|)}{(\frac{q^2}{2\mu_{mm_3}} + \frac{\vec{q}\cdot\vec{p}}{m_3} + \frac{p^2}{2\mu_{mm_3}} - E)}\Delta_2\Delta_3 \quad (\text{A8})$$

$$K_{23}(\vec{p}, \vec{q}; E) = K_{45}(\vec{p}, \vec{q}; E) = K_{ii}(\vec{q}, \vec{p}; E) = 0 \quad (\text{A9})$$

$$K_{i,j}(\vec{p}, \vec{q}; E) = K_{j,i}(\vec{q}, \vec{p}; E), \quad i, j = 1-5 \quad (\text{A10})$$

$$h_1(p) = \int \frac{d\vec{q}[V_{12}^0(q)]^2}{\frac{p^2}{2\mu_{12-3}} + \frac{q^2}{2\mu_{12}} - E}, \quad h_2(p) = \int \frac{d\vec{q}[V_{c23}^0(q)]^2}{\frac{p^2}{2\mu_{23-1}} + \frac{q^2}{2\mu_{23}} - E} \quad (\text{A11})$$

$$h_3(p) = \int \frac{d\vec{q} [V_{c23}^1(q)]^2 (\hat{q} \cdot \hat{p})^2}{\frac{p^2}{2\mu_{23-1}} + \frac{q^2}{2\mu_{23}} - E}, \quad h_4(p) = \int \frac{d\vec{q} [V_{31}^0(q)]^2}{\frac{p^2}{2\mu_{31-2}} + \frac{q^2}{2\mu_{31}} - E} \quad (\text{A12})$$

$$h_5(p) = \int \frac{d\vec{q} [V_{31}^1(q)]^2 (\hat{q} \cdot \hat{p})^2}{\frac{p^2}{2\mu_{31-2}} + \frac{q^2}{2\mu_{31}} - E} \quad (\text{A13})$$

$$\Delta_1 = \frac{\left[\left(\vec{q} \frac{m_3}{m+m_3} + \vec{p} \right) \cdot \hat{q} \right]}{\left[\left(\frac{m_3}{m+m_3} \right)^2 q^2 + p^2 + 2 \frac{m_3}{m+m_3} \vec{q} \cdot \vec{p} \right]^{1/2}} \quad (\text{A14})$$

$$\Delta_2 = \frac{\left[\left(\vec{q} \frac{m}{m+m_3} + \vec{p} \right) \cdot \hat{q} \right]}{\left[\left(\frac{m}{m+m_3} \right)^2 q^2 + p^2 + 2 \frac{m}{m+m_3} \vec{q} \cdot \vec{p} \right]^{1/2}} \quad (\text{A15})$$

$$\Delta_3 = \frac{\left[\left(\vec{p} \frac{m}{m+m_3} + \vec{q} \right) \cdot \hat{p} \right]}{\left[\left(\frac{m}{m+m_3} \right)^2 p^2 + q^2 + 2 \frac{m}{m+m_3} \vec{q} \cdot \vec{p} \right]^{1/2}}. \quad (\text{A16})$$

References

- [1] I Tanihata, *Nucl. Phys.* **A488**, 113c (1988)
- [2] A C Mueller and B M Sherrill, *Annu. Rev. Nucl. Part. Sci.* **43**, 529 (1993)
- [3] M V Zhukov, B V Danilin, D V Fedorov and J M Bang, *Phys. Rep.* **231**, 151 (1993)
- [4] P G Hansen and A J Jensen, *Annu. Rev. Nucl. Part. Sci.* **45**, 591 (1995)
See also a more recent work on the excited state of ^{11}Li by R Kanungo and C Samanta, *J. Phys. G: Nucl. Part. Phys.* **24**, 1611 (1998)
- [5] I Tanihata, *J. Phys. G: Nucl. Part. Phys.* **22**, 157 (1996)
- [6] S Dasgupta, I Majumdar and V S Bhasin, *Phys. Rev.* **C50**, R550 (1994)
See also V S Bhasin, *Pramana -J. Phys.* **53**, 567 (1999)
- [7] T Suzuki and T Otsuka, *Phys. Rev.* **C56**, 847 (1997)
- [8] T Suzuki and T Otsuka, *Phys. Rev.* **C50**, R555 (1994)
- [9] M J G Borge *et al*, *Phys. Rev.* **C55**, R8 (1997)
- [10] T Suzuki, *J. Phys. G: Nucl. Part. Phys.* **24**, 1455 (1998)
- [11] I J Thompson and M V Zhukov, *Phys. Rev.* **C49**, 1904 (1994)
- [12] K Ueta, H Miyake and G W Bund, *Phys. Rev.* **C59**, 1806 (1999)
- [13] I Mukha *et al*, *Nucl. Phys.* **A616**, 201c (1997)
- [14] M J G Borge *et al*, *Nucl. Phys.* **A613**, 199 (1997)
- [15] S Kumar and V S Bhasin, *Phys. Rev.* **C65**, 034007 (2002)
- [16] M V Zhukov, B V Danilin, L V Gregorenko and J S Vaagen, *Phys. Rev.* **C52**, 2461 (1995)
- [17] M Zinser *et al*, *Phys. Rev. Lett.* **75**, 1719 (1995)
- [18] B M Young *et al*, *Phys. Rev.* **C49**, 279 (1994)
- [19] D V Fedorov, A S Jensen and K Riisager, *Phys. Lett.* **B312**, 1 (1993)
- [20] E Garrido, D V Fedorov and A S Jensen, *Nucl. Phys.* **A700**, 117 (2002)
- [21] F Humbert *et al*, *Phys. Lett.* **B347**, 198 (1995)
- [22] P G Hansen, *Nucl. Phys.* **A553**, 89c (1993)

- [23] M G Gornov, Yu. Gurov, S Lapushkin, P Morokhov, V Pechkurov, T K Pedlar, Kamal K Seth, J Wise and D Zhao, *Phys. Rev. Lett.* **81**, 4325 (1998)
- [24] T Myo, K Kato, S Aoyama and K Ikeda, *Phys. Rev.* **C63**, 054313 (2001)
- [25] G Audi and A H Wapstra, *Nucl. Phys.* **A595**, 409 (1995)
- [26] D R Harington, *Phys. Rev.* **B691**, 139 (1965)
- [27] G Cattapan, G Pisent and V Vanzani, *Nucl. Phys.* **A241**, 204 (1975)
- [28] Samuel S M Wong, *Introductory nuclear physics* (Prentice Hall, New Jersey, 1990) p. 106
- [29] I Mukha *et al*, *Phys. Lett.* **B367**, 65 (1996)
- [30] K Rissager, *Nucl. Phys.* **A616**, 169c (1997)
- [31] D Baye and P Descouvemont, *Nucl. Phys.* **A481**, 445 (1988)
- [32] Y Yamaguchi, *Phys. Rev.* **95**, 1628 (1954)
- [33] T Teranishi *et al*, *Phys. Lett.* **B407**, 110 (1997)